Pulmonary vascular morphology as an imaging biomarker in chronic thromboembolic pulmonary hypertension

F. N. Rahaghi,[1] J. C. Ross,[2] M. Agarwal,[1] G. González,[2] C. E. Come,[1] A. A. Diaz,[1] G. Vegas-Sánchez-Ferrero,[2] A. Hunsaker,[2] R. San José Estépar,[2] A. B. Waxman,[1] G. R. Washko[1]

[1]Pulmonary and Critical Care Division, Department of Medicine, Brigham and Women's Hospital, Boston, Massachusetts, USA; [2]Department of Radiology, Harvard School of Medicine, Boston, Massachusetts, USA

Abstract: Patients with chronic thromboembolic pulmonary hypertension (CTEPH) have morphologic changes to the pulmonary vasculature. These include pruning of the distal vessels, dilation of the proximal vessels, and increased vascular tortuosity. Advances in image processing and computer vision enable objective detection and quantification of these processes in clinically acquired computed tomographic (CT) scans. Three-dimensional reconstructions of the pulmonary vasculature were created from the CT angiograms of 18 patients with CTEPH diagnosed using imaging and hemodynamics as well as 15 control patients referred to our Dyspnea Clinic and found to have no evidence of pulmonary vascular disease. Compared to controls, CTEPH patients exhibited greater pruning of the distal vasculature (median density of small-vessel volume: 2.7 [interquartile range (IQR): 2.5–3.0] vs. 3.2 [3.0–3.8]; $P = 0.008$), greater dilation of proximal arteries (median fraction of blood in large arteries: 0.35 [IQR: 0.30–0.41] vs. 0.23 [0.21–0.31]; $P = 0.0005$), and increased tortuosity in the pulmonary arterial tree (median: 4.92% [IQR: 4.85%–5.21%] vs. 4.63% [4.39%–4.92%]; $P = 0.004$). CTEPH was not associated with dilation of proximal veins or increased tortuosity in the venous system. Distal pruning of the vasculature was correlated with the cardiac index ($R = 0.51$, $P = 0.04$). Quantitative models derived from CT scans can be used to measure changes in vascular morphology previously described subjectively in CTEPH. These measurements are also correlated with invasive metrics of pulmonary hemodynamics, suggesting that they may be used to assess disease severity. Further work in a larger cohort may enable the use of such measures as a biomarker for diagnostic, phenotyping, and prognostic purposes.

Keywords: chronic thromboembolic pulmonary hypertension, computed tomography, arterial, tortuosity.

Pulm Circ 2016;6(1):70-81. DOI: 10.1086/685081.

Chronic thromboembolic pulmonary hypertension (CTEPH) is a disease defined by the presence of chronic clot accompanied by vascular remodeling and pulmonary arterial hypertension.[1-5] Despite the introduction of pharmacologic therapies for CTEPH,[6] pulmonary thromboendarterectomy (PTE) remains the gold-standard treatment for advanced, symptomatic disease.[1] While imaging is important for both the diagnosis of CTEPH and evaluation for PTE,[7,8] interpretation of vascular morphology remains challenging. Features such as pruning of the distal vasculature, dilation of the more central vasculature, and vessel tortuosity have all been reported, yet there are few published data on objective assessments of these processes in patients with CTEPH.[8-10]

Advances in computer vision have facilitated complex volumetric assessments of intraparenchymal vascular morphology.[11,12] Such efforts enable quantification of vasculature for utilization in clinical, epidemiologic, and genetic investigation. We sought to objectively assess vascular morphology in patients with CTEPH, compare these measures to those in a cohort of well-characterized controls, and preliminarily examine their hemodynamic correlates.

METHODS

A sequential cohort of 390 patients who were referred to Brigham and Women's Hospital for evaluation of unexplained dyspnea and underwent right heart catheterization (RHC) was retrospectively reviewed to identify patients with CTEPH. Evidence of chronic thrombus on computed tomography pulmonary angiogram (CTPA) plus pulmonary hypertension on RHC was the initial criterion for inclusion; subjects also had to have a CTPA within 1 year of RHC and before thromboendarterectomy. This group was designated the CTEPH subgroup. A group of subjects without any evidence of lung disease by CTPA and pulmonary-function testing and with normal resting RHC measurements was selected as the control group.

Electronic chart review was used to verify demographic and hemodynamic information. All RHCs were performed by the same team; only resting hemodynamic measurements were used in this investigation. Stroke volume was calculated by dividing cardiac output by heart rate; pulmonary arterial compliance was estimated as stroke volume divided by pulse pressure.[13] Computed tomography (CT) image processing was performed as described previously.[11,12]

Address correspondence to Dr. F. N. Rahaghi, Brigham and Women's Hospital, Pulmonary and Critical Care Division, Department of Medicine, 75 Francis Street, PBB–CA 3, Boston, MA 02115. E-mail: frahaghi@partners.org.

Submitted September 10, 2015; Accepted December 1, 2015; Electronically published February 3, 2016.

Briefly, the lungs and lobes were segmented, and a 3-dimensional (3D) reconstruction of the intraparenchymal vasculature was generated. Following visual inspection of these 3D reconstructions, blood vessel volume was reported as a function of vascular cross-sectional area. For example, BV5 is the blood vessel volume for all vessels in a region of interest (lung or lobe) with a cross-sectional area of ≤ 5 mm^2, while BV>10 is the blood vessel volume for all vessels >10 mm^2 in cross section. These cutoffs were selected on the basis of prior work quantifying vascular pruning on CT scan and the hypothesis that, in addition to pruning, there may be consequent dilation of the more central vessels.[12,14,15] The total blood vessel volume (TBV) is the total volume of the intraparenchymal pulmonary vasculature in the region of interest. To normalize blood vessel volume across the study cohort, two indices were computed: (1) BV5 and BV>10 divided by the volume of the lung or lobe from which the measure was calculated (ρBV5 and ρBV>10, respectively) and (2) BV5 and BV>10 divided by the TBV of the region of interest (BV5/TBV and BV>10/TBV, respectively).

The minimum-spanning-tree model ("Minimum spanning tree," available online) was used to divide the vasculature into individual segments based on branching points. These segments were traced back to the segmental pulmonary arteries and veins and manually labeled to create an arterial-venous (AV)-segmented label map ("AV segmentation," available online). These segments were also used to compute central tortuosity ("Tortuosity," available online). The median vessel segment tortuosity was assessed for each region of interest.

Logistic-regression models and receiver operating curve (ROC) generation were performed with STATA 14 (StataCorp, College Station, TX). All other statistical analyses were performed with SAS 9.3 (SAS Institute, Cary, NC). Continuous variables are presented as medians and interquartile ranges, dichotomous variables as numbers or proportions. Nonparametric statistics were employed, specifically the Wilcoxon rank-sum test for comparing the CTEPH and control cohorts, Spearman correlation for evaluating relationships between variables, and the Fisher exact test for comparing proportions by gender. Two-sided P values were reported for all comparisons; P values of <0.05 were considered significant. All participants had previously signed informed consent for the secondary analysis of their clinical data. This protocol was approved by the Institutional Review Board of Brigham and Women's Hospital.

RESULTS

Chart review resulted in the identification of 18 patients with CTEPH and 15 controls, with median times of 2 (CTEPH) and 42 (control) days between imaging and RHC. Demographic information and baseline hemodynamic measures for each group are shown in Table 1. The groups were well matched by age, with a nonsignificant trend for more females in the control group. As expected, the pulmonary artery pressure and pulmonary vascular resistance (PVR) were significantly higher in the CTEPH group than in the control group (medians: 52.0 vs. 15.0 mmHg and 10.6 vs. 1.01 Wood units, respectively; $P < 0.001$ for both comparisons), while cardiac index (CI) was lower in the CTEPH group (1.98 vs. 2.95, $P < 0.001$).

Intraparenchymal pulmonary vascular segmentation was successfully performed in all lobes of all 33 subjects. Visual inspection of the 3D models of the pulmonary vasculature revealed marked

Table 1. Demographics and baseline hemodynamics of the two cohorts studied

	CTEPH cohort ($N = 18$)	Control cohort ($N = 15$)	P value[a]
Demographics			
Age, years	51.0 (44.0–64.0)	46 (42.0–61.0)	0.77
Female sex, no.	7	10	0.17
Resting hemodynamics			
Mean PA pressure, mmHg	52.0 (38.0–66.0)	15.0 (12.0–18.0)	<0.001
Wedge pressure, mmHg	11.0 (10.0–12.0)	8.0 (7.0–12.0)	0.17
Cardiac index	1.98 (1.66–2.68)	2.95 (2.63–3.4)	<0.001
PVR, Wood units	10.6 (0.66–17.3)	1.01 (0.85–1.64)	<0.001
RA pressure, mmHg	14.0 (11.0–16.0)	5.0 (3.0–8.0)	<0.001
Stroke volume, mL	50.0 (32.9–77.9)	79.3 (65.8–92.5)	0.02
Compliance	0.84 (0.61–1.56)	5.7 (4.64–7.53)	<0.001

Note: Data are reported as median (interquartile range) unless otherwise specified. CTEPH: chronic thromboembolic pulmonary hypertension; PA; pulmonary arterial; PVR: pulmonary vascular resistance; RA: right atrial.

[a] P values were computed on the basis of a Wilcoxon 2-sample exact test with a 2-sided P value, with the exception of gender proportions, which were compared using the Fisher exact test.

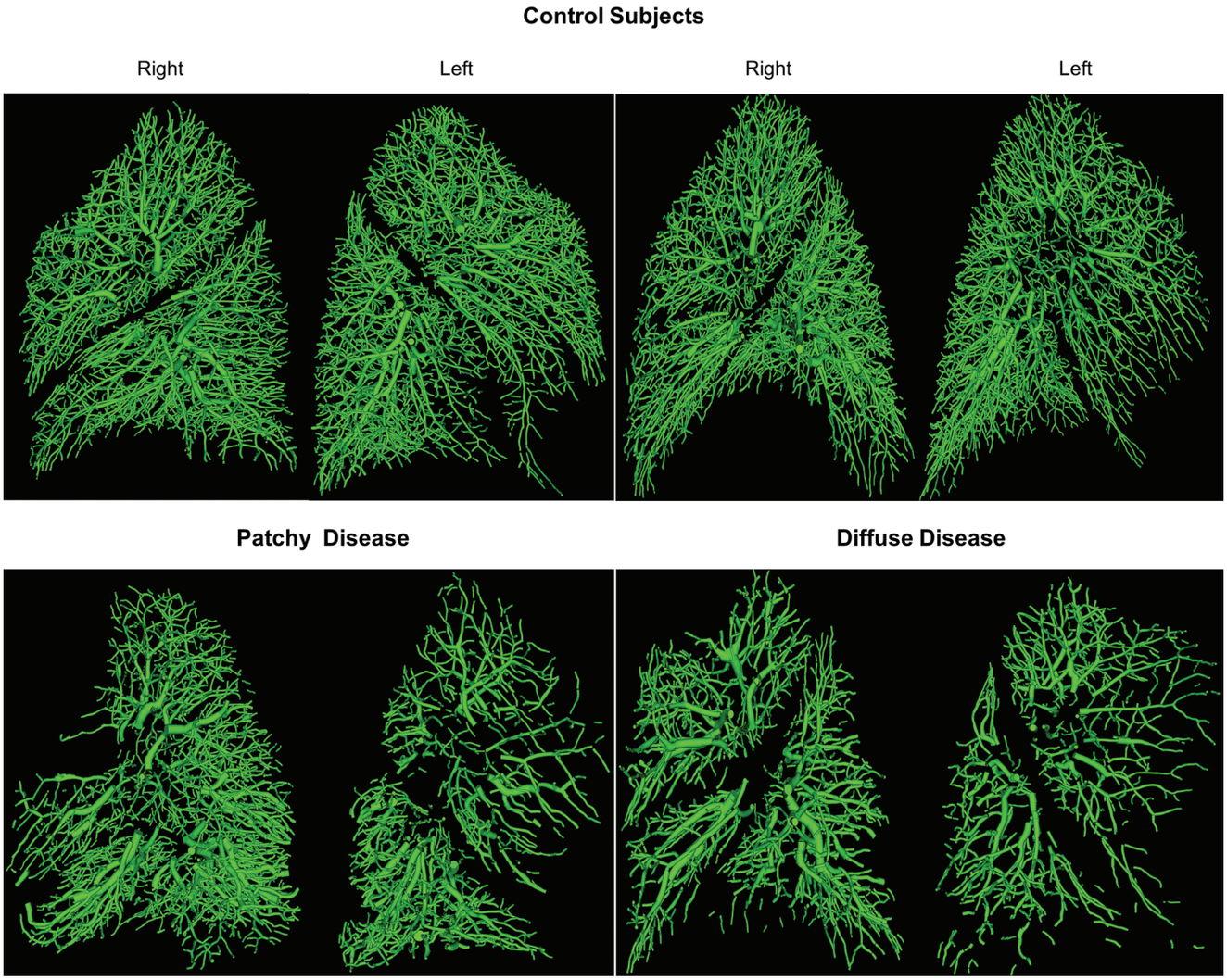

Figure 1. Examples of vascular reconstruction for 2 control subjects (*top*) and 2 patients with chronic thromboembolic pulmonary hypertension (*bottom*). Some patients exhibited patchy disease (*bottom left*), whereas others exhibited diffuse disease throughout the vascular tree (*bottom right*).

differences between the controls and those with CTEPH as well as within the CTEPH patients themselves. One of the more striking subjective features detected on this inspection was pruning of the distal vasculature and its regional variability (Fig. 1).

To quantify this vascular pruning and enable correlative investigation, we created aggregate plots of blood vessel volume versus vascular cross-sectional area for lungs and lobes of interest (Fig. 2). From these plots we calculated BV5/TBV and ρBV5. There was no difference in TBV between the CTEPH and control groups. However, global as well as right- and left-lung BV5/TBV and ρBV5 were decreased in the CTEPH patients (BV5/TBV: 0.58 vs. 0.45, P = 0.0007 globally, 0.59 vs. 0.47, P = 0.001 for right lung, 0.57 vs. 0.41, P = 0.0009 for left lung; ρBV5: 3.2 vs. 2.7, P = 0.008 globally, 3.2 vs. 2.9, P = 0.04 for right lung, 3.1 vs. 2.5, P = 0.002 for left lung), consistent with distal pruning (Table 2). Lobar analysis of the same quantities similarly showed that BV5/TBV and ρBV5 also tended to be reduced in CTEPH patients (Table S1; Tables S1 and S2 are available online).

The volume-versus–vessel cross-sectional area plots also revealed a shift of the blood volume to larger vessels. Both BV>10/TBV and ρBV>10 were increased in patients with CTEPH (0.35 vs. 0.28, P = 0.0009 and 2.5 vs. 1.8, P = 0.008, respectively). This was true for all global (Table 2) and regional (Table S1) measures, with the exception of ρBV>10 from the right middle lobe (P = 0.06).

All reconstructed vasculature was then segmented into arteries and veins (Fig. 3). The arterial small-vessel fraction ($BV5_{ART}/TBV_{ART}$) was decreased globally (Table 3), by lung, and by lobe (Table S2) in CTEPH subjects, compared with controls. The venous small-vessel fraction ($BV5_{VEIN}/TBV_{VEIN}$) was significantly lower in CTEPH than in control subjects in only 3 of the 5 lobes (Table S2).

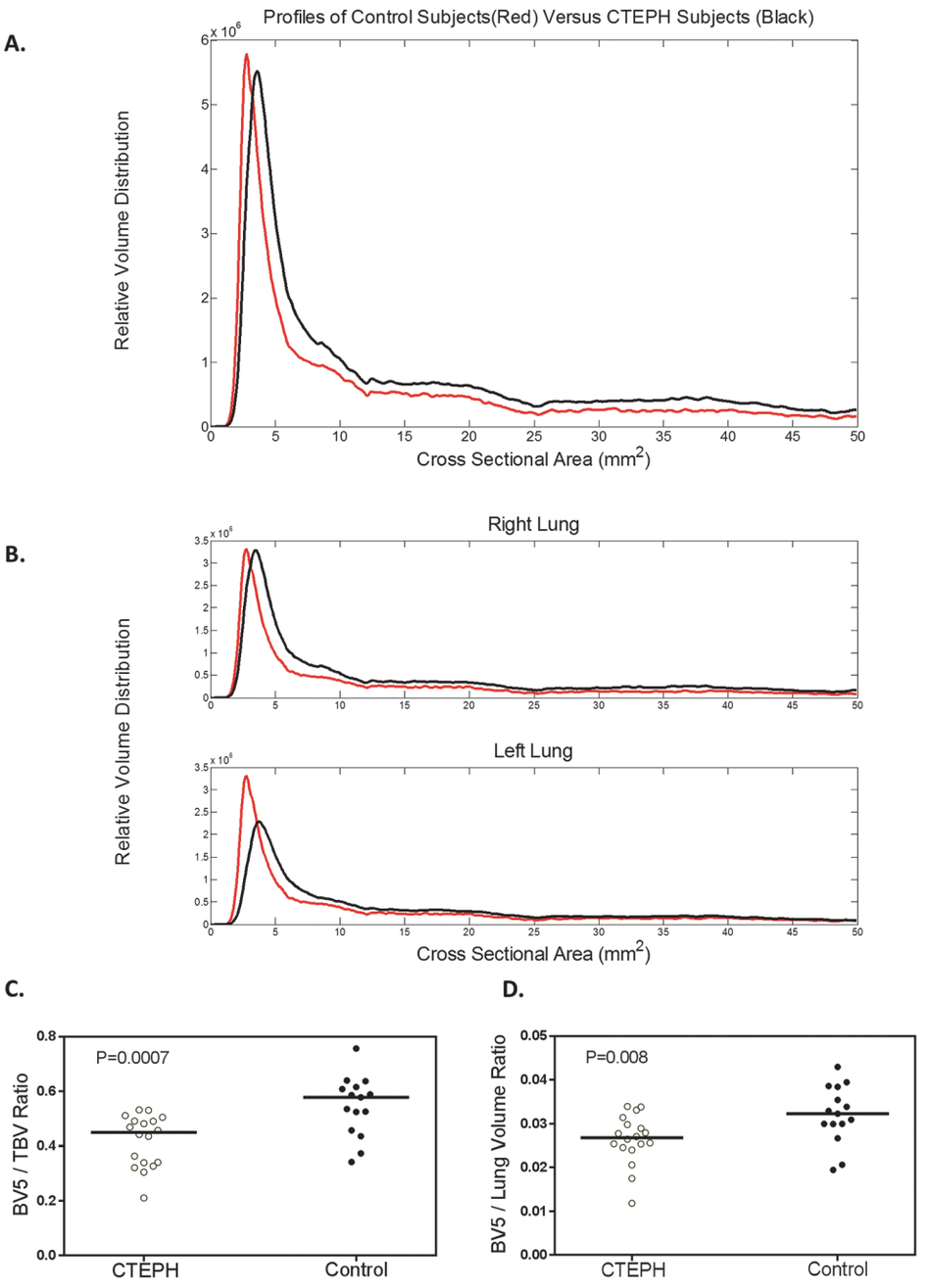

Figure 2. Volume distribution profiles for CTEPH and control subjects. *A*, Whole-lung profile. Note the rightward and downward shift of the peak for subjects with CTEPH, indicating loss of small vasculature. *B*, Individual lung profiles. *C*, *D*, The two computed measures of small-vessel loss, the small-vessel volume fraction BV5/TBV (*C*) and small-vessel volume density ρBV5 (*D*). BV5: blood vessel volume for vessels with a cross-sectional area ≤ 5 mm^2; CTEPH: chronic thromboembolic pulmonary hypertension; TBV: total blood vessel volume; ρBV5: BV5/lung volume.

In the larger vessels, the global and lobar arterial large-vessel fractions ($BV{>}10_{ART}/TBV_{ART}$) were increased in CTEPH relative to controls, but no similar change was seen in the venous phase ($BV{>}10_{VEIN}/TBV_{VEIN}$).

The arterial/venous ratio of the TBV (TBV_{ART}/TBV_{VEIN}) was increased in the CTEPH versus the control group (1.41 vs. 1.09, $P = 0.002$; Table 3). The same phenomenon was observed when the analysis was limited to vessels with a cross-sectional area >10 mm^2 ($BV{>}10_{ART}/BV{>}10_{VEIN}$) at the global, single-lung, and lobar levels (with the exception of the right middle lobe). There was no difference, however, in the arterial/venous BV5 ratio ($BV5_{ART}/BV5_{VEIN}$) between the two groups. These findings are illustrated in Figure 3.

Table 2. Comparison of image-derived volumes and metrics of small-vessel density as well as regional density measures in CTEPH and control groups

	CTEPH	Control	*P* value[a]
Lung volume, L			
Right lung	2.16 (1.44–2.63)	1.87 (1.59–2.32)	0.58
Left lung	1.5 (1.25–2.15)	1.76 (1.32–2.07)	0.73
Total blood volume density TBV/lung volume, mL vessel/dL lung			
Whole lung	6.0 (5.6–7.2)	6.0 (4.9–6.7)	0.38
Right lung	6.4 (5.6–7.3)	5.9 (4.9–6.8)	0.26
Left lung	6.1 (5.6–7.1)	5.9 (4.8–7.1)	0.49
Small-vessel volume fraction, BV5/TBV			
Whole lung	0.45 (0.34–0.49)	0.58 (0.46–0.62)	0.0007
Right lung	0.47 (0.38–0.53)	0.59 (0.54–0.64)	0.0010
Left lung	0.41 (0.27–0.46)	0.57 (0.47–0.62)	0.0009
Large-vessel volume fraction, BV>10/TBV			
Whole lung	0.35 (0.32–0.40)	0.28 (0.24–0.34)	0.0009
Right lung	0.34 (0.31–0.45)	0.26 (0.24–0.29)	0.0006
Left lung	0.36 (0.33–0.43)	0.29 (0.24–0.33)	0.002
Small-vessel density ρBV5, mL vessel/dL lung			
Whole lung	2.7 (2.5–3.0)	3.2 (3.0–3.8)	0.008
Right lung	2.9 (2.5–3.3)	3.2 (3.1–3.9)	0.04
Left lung	2.5 (2.0–2.8)	3.1 (2.7–3.7)	0.002
Large-vessel density ρBV>10, mL vessel/dL lung			
Whole lung	2.5 (1.8–2.8)	1.8 (1.4–2.0)	0.008
Right lung	2.4 (1.7–2.8)	1.7 (1.2–2.1)	0.006
Left lung	2.5 (1.8–2.9)	1.6 (1.5–2.2)	0.009

Note: Data reported as median (interquartile range). BV>10: volume of vessels with cross-sectional area > 10 mm^2. BV5: volume of vessels with cross-sectional area ≤ 5 mm^2; CTEPH: chronic thromboembolic pulmonary hypertension; TBV: total volume of blood vessels detected; ρBV5: BV5/total lung volume; ρBV>10: BV>10/total lung volume.

[a] *P* value based on a Wilcoxon exact test with a 2-sided *P* value.

Using the vessel segments generated by fitting of the minimum spanning tree, we then calculated the tortuosity of the arterial and venous pulmonary vasculature (Fig. 4). Whole-lung arterial tortuosity was significantly increased in the CTEPH subjects, compared to controls (4.92% vs. 4.63%, $P = 0.0035$; Table 4). While there were associations between the tortuosity metric and both the segment length and vessel diameter, visual inspection of the plots suggest that arterial tortuosity in the CTEPH patients was consistently higher than that in controls (Fig. 4, *bottom*). There was no relationship between the number of vessel segments detected and tortuosity ($R = -0.24$, $P = 0.18$ for the arterial tree and $R = -0.09$, $P = 0.29$ for the venous tree). We then examined the associations between these CT vascular measures and hemodynamics obtained by RHC in the patients with CTEPH (Table 5). There was generally no association between small- or large-vessel volume fractions (BV5/TBV or BV>10/TBV) and hemodynamics. Both the global and right-lung measures of ρBV5, however, were directly associated with higher cardiac indices and estimated stroke volumes. The right-lung ρBV5 was further associated with higher estimated vascular compliance ($R = 0.62$, $P = 0.01$) and lower PVR ($R = -0.66$, $P = 0.006$). The correlation was strongest with values obtained from the right upper lobe. There were no statistically significant associations between the left-lung ρBV5 and hemodynamic parameters.

In the AV-segmented vasculature, we focused on the TBV_{ART}/TBV_{VEIN} and the $BV{>}10_{ART}/BV{>}10_{VEIN}$, which were demonstrated to be increased in CTEPH patients, compared to controls. The TBV_{ART}/TBV_{VEIN} and $BV{>}10_{ART}/BV{>}10_{VEIN}$ were directly related to right atrial pressure, but there were no other statistically significant associations between global arterial/venous ratios and other hemodynamic parameters. Vascular tortuosity (whether total, arterial, or venous) was not associated with RHC data.

DISCUSSION

Thromboembolic disease is often characterized by heterogeneous pulmonary vascular disease leading to a characteristic "moth-eaten" appearance on perfusion scans. On CT scan, this disease may visually manifested as pruning of the distal vasculature, dilation of the central pulmonary arteries, and tortuous-appearing vessels. In this study, we used a computer-generated 3D model of the pulmonary vasculature to derive imaging-based biomarkers for these observations. Our objective assessments of intraparenchymal pulmonary vasculature corroborate these previous subjective findings, demonstrating that patients with CTEPH have measurably smaller distal vasculature, engorgement of the central vasculature, and asymmetry in the arterial and venous vascular beds. Patients with CTEPH also have increased tortuosity in the pulmonary arteries.

Pruning of the distal vasculature was quantitatively assessed by two indices, BV5/TBV and ρBV5. Normalization for blood volume or lung volume was performed to make our vascular measures independent of anthropomorphics, such as body size, that would affect absolute lung and blood vessel volume. Both of these measures were reduced in CTEPH patients, a finding that may be due to a combination of vascular remodeling, diminished lumen size, and decreased regional perfusion. In the case of BV5/TBV, both engorgement of the proximal vessels and loss of detection of distal vasculature could decrease this quantity. For ρBV5, loss of perfusion with associated luminal narrowing may lead to a decreased number of detected small vessels. While both types of biomarkers appeared to be relatively similar in their ability to discriminate CTEPH patients from controls,

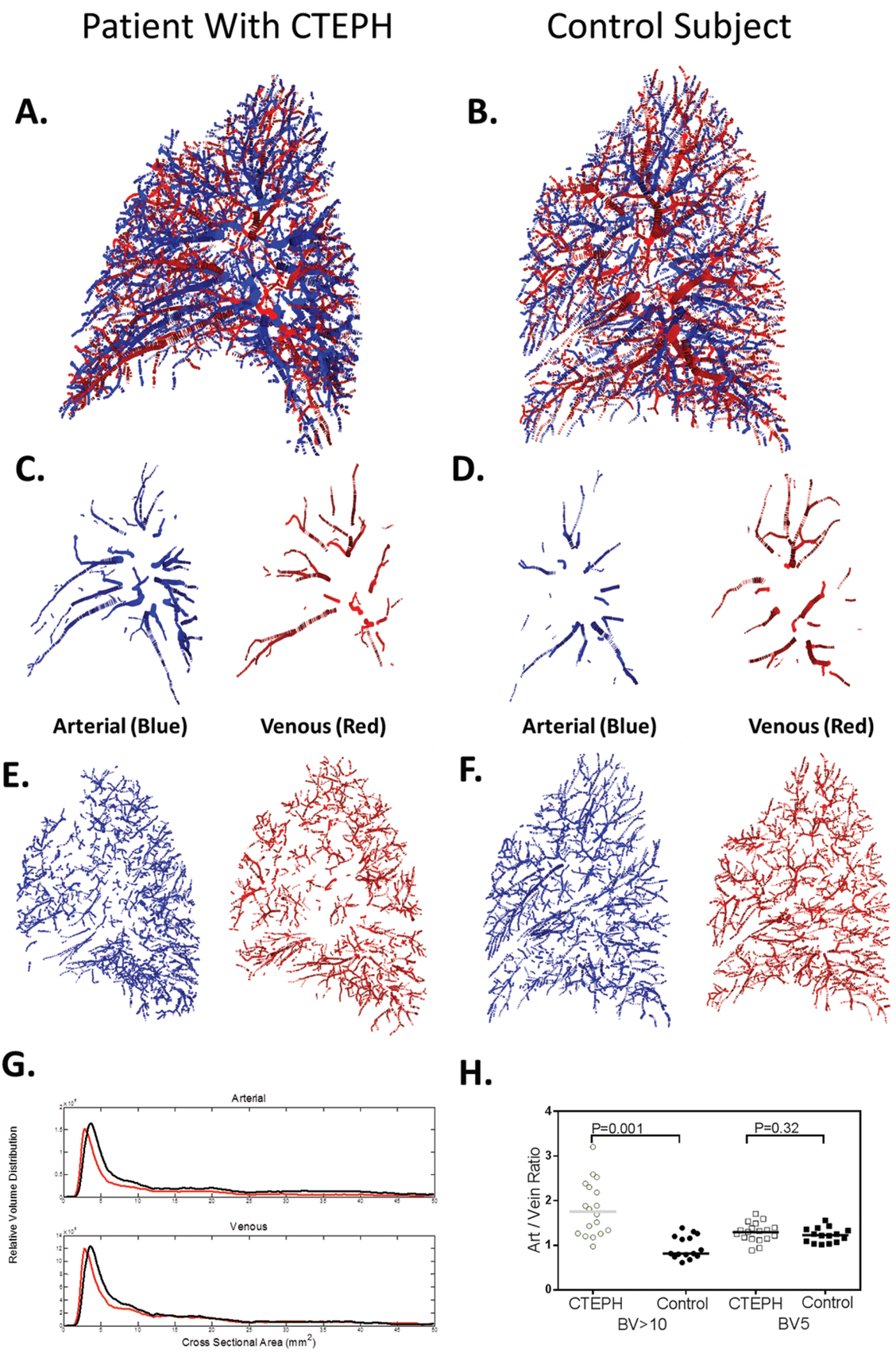
Patient With CTEPH
Control Subject
A.
B.
C.
D.
Arterial (Blue)
Venous (Red)
Arterial (Blue)
Venous (Red)
E.
F.
G.
Arterial
Venous
Relative Volume Distribution
Cross Sectional Area (mm2)
H.
P=0.001
P=0.32
Art / Vein Ratio
CTEPH
Control
CTEPH
Control
BV>10
BV5

only the latter measure of small-vessel density provided statistically significant correlations with invasive hemodynamic measures. The direction of this correlation suggests that reductions in BV5 due to either narrowing of existing vessels or absolute loss of vasculature are associated with an increased PVR.

AV segmentation revealed that distal pruning had both an arterial and a venous component, although the latter was not significant in all lobes and likely represents a smaller effect. Precapillary arterial pruning may be due to remodeling of the distal vasculature in the presence of chronic thrombus and decreased flow, while the apparent decreases in the distal venous vasculature may represent diminished regional blood flow downstream from these changes.

Our assessments of the intraparenchymal pulmonary vasculature also included measures focused on the quantification of the more proximal vessel engorgement. These measures, BV>10/TBV and ρBV>10, were generally increased in CTEPH patients, compared to our control cohort. Further separating arterial and venous vessels revealed that this was an arterial effect. The CTEPH patients had an increased total blood volume arterial/venous ratio (TBV_{ART}/TBV_{VEIN}) as well as differential arterial engorgement of the central vessels whose caliber was >10 mm^2 ($BV{>}10_{ART}/BV{>}10_{VEIN}$). This suggests that increases in these ratios may be due to arterial dilatation secondary to local thrombus and/or increased regional PVR.

Tortuosity is a phenomenon commonly observed with hypertension in the systemic circulation.[16-19] It has also been observed in the pulmonary circulation and has been shown to be increased in patients with pulmonary arterial hypertension.[20] Prior literature has attempted to quantify these observations with a number of different techniques, but the simplest measurement relies on comparing the direct path versus the actual path a vessel takes between two endpoints.[16,20] Using this approach, we found that the group with CTEPH had increased tortuosity in the arterial system. Tortuosity could be caused by collapse of the lung as well as by adaptation and remodeling in the face of increased arterial pressures. Given the more compliant nature of the venous system, one would expect greater lung volume effects in this vascular bed. We found, however, greater tortuosity in the arterial system, suggesting that these changes are a reflection of vascular pathology and not of the surrounding lung.

To examine the ability of these morphological parameters to distinguish patients with CTEPH from controls, we constructed a logistic-regression model, using four parameters derived from whole-lung values: the small-vessel fraction (BV5/TBV), the vascular density (ρBV5), the arterial/venous ratio of the larger vessels ($BV{>}10_{ART}/BV{>}10_{VEIN}$), and the tortuosity of the arterial system. The individual and combined ROCs are shown in Figure 5. The individual performances of the models all show an area under the curve of >0.7, but the $BV{>}10_{ART}/BV{>}10_{VEIN}$ demonstrates the best discriminatory potential. Combining these four parameters leads to an improved prediction model, shown in Figure 5*E*. The results of these analyses must be interpreted with caution, however, given that these subjects may not be typical representatives of patients undergoing diagnostic evaluation for the presence of CTEPH.

This investigation is limited by the retrospective nature of the data, combined with a lack of appropriate imaging data for some CTEPH patients who otherwise could have been included in the study. Without prospective design, variations in the specific imaging protocols used likely served as a significant source of variability in each group, although statistically significant differences were detected. Further investigation in a larger cohort, using prospectively acquired images, will be needed to substantiate our findings. Further, the CT and RHC data used for correlative studies were not obtained on the same day, although the median 2-day difference between the two in the CTEPH patients suggests that the risk of an intercurrent process selectively affecting one of these is low. Finally, our control cohort may not have been free of cardiopulmonary disease. These subjects were referred for clinical evaluation because of unexplained dyspnea and may have been suffering from an occult process. Despite this possibility, our entire control cohort had normal pulmonary vascular measures on invasive hemodynamic assessment and no subjective evidence of cardiopulmonary disease on CT scan.

In this study, we measured markers of distal-vessel pruning, proximal-vessel dilation, differential distribution of volume between arterial and venous beds, and changes in vessel tortuosity. We have shown that these biomarkers differ significantly between patients with CTEPH and controls and that they correlate with invasive hemodynamic measurements. Our lobar data further suggest that vascular metrics may provide insight into the regionality of disease that may complement aggregate measures such as echocardiography and RHC. Further work is needed to determine whether such objective methods could be used for diagnostic purposes, such as distinguishing patients with CTEPH from patients with acute pulmonary embolism, or for therapeutic planning.

Figure 3. *A*, *B*, Example of an arterial-venous-segmented vascular tree is shown for a patient with CTEPH (*A*) and a control subject (*B*), with the arterial phase shown in blue and the venous phase shown in red. *C–F*, The proximal vasculature (*C*, *D*) and the distal vasculature (*E*, *F*), separated by size, are shown under the respective images. Note the loss of smaller vessels in *E*, in comparison with *F*, and the dilation of the large proximal vasculature in the arterial, as compared to venous, proximal vessels in *C*. *G*, Relative volume distribution profiles combined for each cohort for both the arterial (*top*) and venous (*bottom*) phases. Note the rightward shift of the vascular profile in the subjects with CTEPH (black lines) compared to controls (red lines), as also demonstrated in Figure 2. In the arterial system, the CTEPH cohort also has increased distribution in the large vessels (cross-sectional area > 10 mm^2). *H*, Comparisons of large vessels (BV>10) and small vessels (BV5) are shown for both groups, highlighting the difference in arterial/venous (Art/Vein) ratios in the two different vessel sizes. BV5: blood vessel volume for vessels with a cross-sectional area ≤ 5 mm^2; BV>10: blood vessel volume for vessels with a cross-sectional area > 10 mm^2; CTEPH: chronic thromboembolic pulmonary hypertension.

Table 3. Comparison of image-derived volumes and metrics of small-vessel arterial and venous volume fractions and arterial/venous ratios for CTEPH and control groups

	CTEPH	Control	*P* value[a]
Arterial fractions			
Small vessels, $BV5_{ART}/TBV_{ART}$			
Whole lung	0.46 (0.32–0.52)	0.60 (0.50–0.64)	0.0005
Right lung	0.49 (0.37–0.55)	0.61 (0.52–0.66)	0.0009
Left lung	0.40 (0.29–0.46)	0.59 (0.50–0.67)	0.001
Large vessels, $BV>10_{ART}/TBV_{ART}$			
Whole lung	0.35 (0.30–0.41)	0.23 (0.21–0.31)	0.0005
Right lung	0.32 (0.30–0.36)	0.23 (0.19–0.29)	0.0002
Left lung	0.35 (0.32–0.41)	0.24 (0.21–0.31)	0.0009
Venous fractions			
Small vessels, $BV5_{VEIN}/TBV_{VEIN}$			
Whole lung	0.48 (0.39–0.52)	0.53 (0.46–0.62)	0.07
Right lung	0.51 (0.40–0.54)	0.54 (0.49–0.59)	0.086
Left lung	0.45 (0.32–0.49)	0.51 (0.44–0.57)	0.027
Large vessels, $BV>10_{VEIN}/TBV_{VEIN}$			
Whole lung	0.28 (0.26–0.32)	0.29 (0.27–0.34)	0.6
Right lung	0.28 (0.26–0.32)	0.27 (0.26–0.32)	0.93
Left lung	0.28 (0.26–0.32)	0.30 (0.25–0.34)	0.66
Arterial/venous ratios			
Small vessels, $BV5_{ART}/BV5_{VEIN}$			
Whole lung	1.31 (1.15–1.39)	1.22 (1.07–1.36)	0.32
Right lung	1.24 (1.10–1.52)	1.22 (1.09–1.45)	0.76
Left lung	1.33 (1.11–1.44)	1.24 (1.03–1.31)	0.06
Large vessels, $BV>10_{ART}/BV>10_{VEIN}$			
Whole lung	1.75 (1.26–2.3)	0.82 (0.76–1.20)	<0.001
Right lung	1.52 (1.2–2.15)	0.85 (0.68–1.15)	<0.0001
Left lung	1.97 (1.31–2.65)	0.90 (0.76–1.24)	0.0001
Overall, TBV_{ART}/TBV_{VEIN}			
Whole lung	1.41 (1.16–1.59)	1.09 (0.97–1.19)	0.002
Right lung	1.34 (1.11–1.51)	1.09 (1.01–1.22)	0.044
Left lung	1.45 (1.24–1.8)	1.05 (1.0–1.22)	0.0005

Note: Data reported as median (interquartile range). BV5: volume of vessels detected with cross sectional area ≤ 5 mm^2 (small vessels); BV>10: volume of vessels detected with cross sectional area > 10 mm^2; CTEPH: chronic thromboembolic pulmonary hypertension; TBV: total volume of vessels detected.

[a] *P* value based on a Wilcoxon exact test with a 2-sided *P* value.

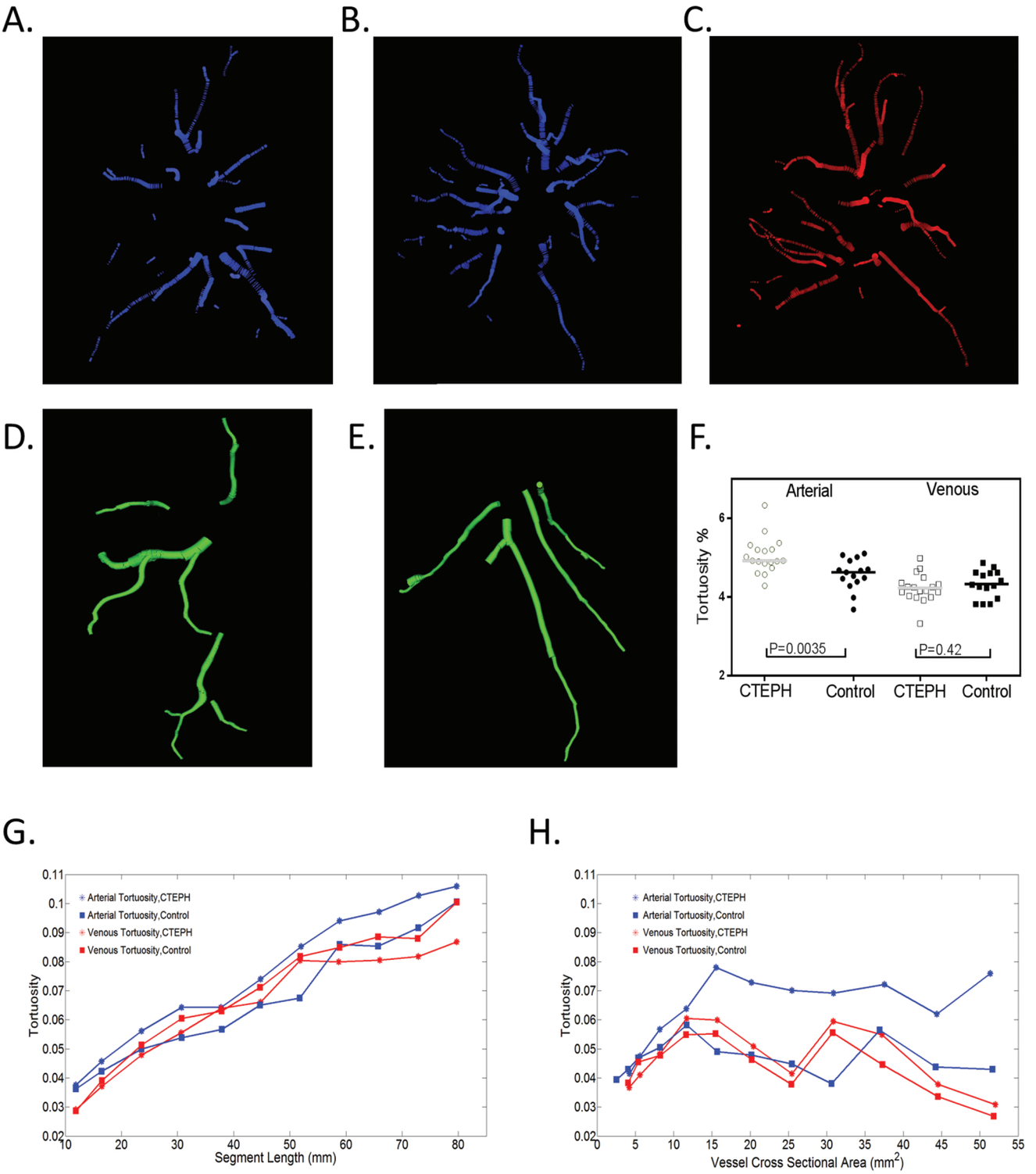

Figure 4. *A*, *B*, Examples of the right-lung proximal arterial vasculature in a control (*A*) and a patient with CTEPH and evidence of increased tortuosity (*B*). *C*, The proximal venous system, with less-tortuous vessels in the same CTEPH patient. *D*, *E*, The most tortuous arterial (*D*) and venous (*E*) proximal vessels in the right lower lobe of another patient with CTEPH, illustrating the significant tortuosity in the arterial but not the venous system. Proximal vessels are shown for ease of visualization. *F*, Comparison between the CTEPH and control cohorts. *G*, *H*, Relationships between segment tortuosity and segment length (*G*) and between segment tortuosity and segment cross-sectional area (*H*). Note that arterial tortuosity in CTEPH remains higher than arterial tortuosity in controls and venous tortuosity in both groups. CTEPH: chronic thromboembolic pulmonary hypertension.

Table 4. Comparison of image derived tortuosity in CTEPH and control groups

	CTEPH	Control	*P* value[a]
Median segmental tortuosity, arterial			
Whole lung	4.92 (4.85–5.21)	4.63 (4.39–4.92)	0.0035
Right lung	4.85 (4.75–5.2)	4.65 (4.3–4.86)	0.052
Left lung	5.04 (4.69–5.46)	4.75 (4.3–4.83)	0.015
Median segmental tortuosity, venous			
Whole lung	4.2 (4.03–4.36)	4.3 (3.96–4.62)	0.42
Right lung	4.28 (4.15–4.41)	4.24 (3.86–4.6)	0.85
Left lung	4.27 (3.94–4.49)	4.34 (4.11–4.65)	0.34
No. of vessel segments used			
Right lung, arterial	499 (244–704)	534 (388–620)	0.73
Left lung, arterial	305 (266–487)	417 (369–515)	0.18
Right lung, venous	420 (270–525)	432 (357–589)	0.41
Left lung, venous	259 (184–361)	384 (292–474)	0.03

Note: Data reported as median (interquartile range). CTEPH: chronic thromboembolic pulmonary hypertension.

[a] *P* value based on a Wilcoxon exact test with a 2-sided *P* value.

Table 5. Correlation of metrics of small-vessel density with hemodynamic measures

	Whole-lung ρBV5	Right-lung ρBV5	RUL ρBV5	A/V BV>10
Cardiac index	0.51 (0.04)	0.7 (0.003)	0.55 (0.03)	. . .
PVR	. . .	−0.66 (0.006)	−0.70 (0.003)	. . .
Mean PAP	. . .	. . .	−0.42 (0.08)	0.33 (0.18)
Systolic PAP	. . .	. . .	. . .	0.38 (0.13)
Diastolic PAP	. . .	. . .	−0.56 (0.02)	. . .
Wedge pressure	. . .	. . .	. . .	. . .
RAP	. . .	. . .	. . .	0.58 (0.01)
Stroke volume	0.48 (0.06)	0.73 (0.001)	0.69 (0.003)	. . .
Compliance	. . .	0.62 (0.01)	0.65 (0.008)	. . .

Note: Data reported as *R* value (*P* value). Ellipses indicate correlation coefficients with $P > 0.1$. A/V BV>10: arterial/venous ratio of the volume of vessels with cross-sectional area > 10 mm^2; BV5: volume of vessels with cross-sectional area ≤ 5 mm^2; PAP: pulmonary arterial pressure; PVR: pulmonary vascular resistance; RAP: right atrial pressure; RUL: right lung, upper lobe; ρBV5: BV5/total lung volume.

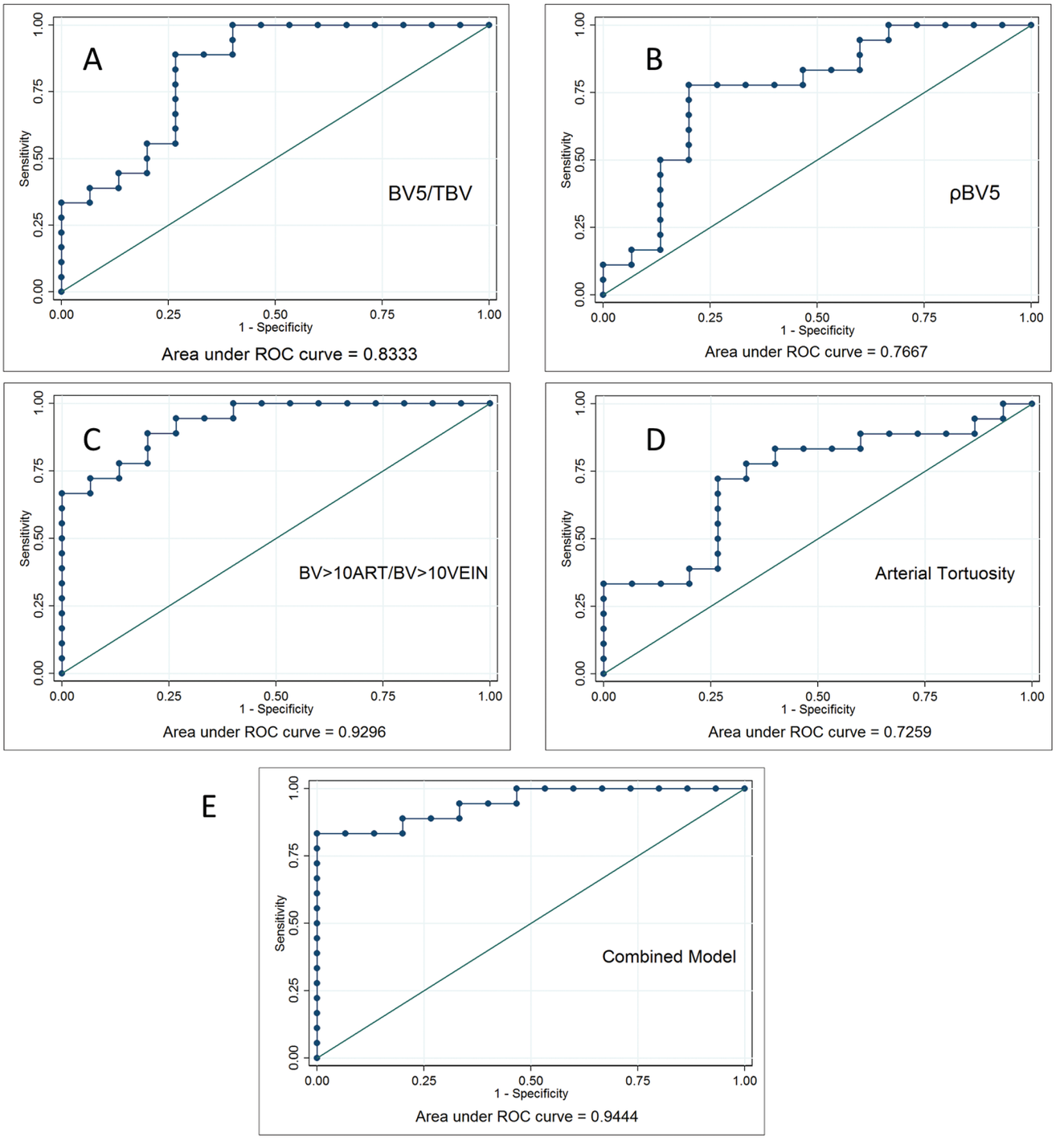

Figure 5. *A–D*, Logistic regression–based receiver operating curves (ROCs) based on four of the key morphologic measures distinguishing CTEPH and control subjects (combined whole lungs): BV5/TBV (*A*), ρBV5 (*B*), $BV{>}10_{ART}/BV{>}10_{VEIN}$(*C*), and arterial tortuosity (*D*). Of these, the arterial/venous ratio of the larger vessels has the strongest discriminating ability, as measured by the area under the curve. *E*, Model combining all four parameters. BV5: blood vessel volume for vessels with a cross-sectional area $\leq$ 5 mm^2; BV>10: blood vessel volume for vessels with a cross-sectional area > 10 mm^2; CTEPH: chronic thromboembolic pulmonary hypertension; TBV: total blood vessel volume; ρBV5: BV5/lung volume.

Source of Support: Authors in this study were supported by National Heart, Lung, and Blood Institute grants 5T32HL007633 (FNR) and 1R01HL116931 (RSJE and GRW).

Conflict of Interest: None declared.

REFERENCES

1. Morris TA. Why acute pulmonary embolism becomes chronic thromboembolic pulmonary hypertension: clinical and genetic insights. Curr Opin Pulm Med 2013;19(5):422–429.
2. Delcroix M, Vonk Noordegraaf A, Fadel E, Lang I, Simonneau G, Naeije R. Vascular and right ventricular remodelling in chronic thromboembolic pulmonary hypertension. Eur Respir J 2013;41(1):224–232.
3. Quarck R, Wynants M, Ronisz A, Sepulveda MR, Wuytack F, Van Raemdonck D, Meyns B, Delcroix M. Characterization of proximal pulmonary arterial cells from chronic thromboembolic pulmonary hypertension patients. Respir Res 2012;13:27. doi:10.1186/1465-9921-13-27.
4. Alias S, Redwan B, Panzenböck A, Winter MP, Schubert U, Voswinckel R, Frey MK, et al. Defective angiogenesis delays thrombus resolution: a potential pathogenetic mechanism underlying chronic thromboembolic pulmonary hypertension. Arterioscler Thromb Vasc Biol 2014;34(4):810–819.
5. Alias S, Lang IM. Coagulation and the vessel wall in pulmonary embolism. Pulm Circ 2013;3(4):728–738.
6. Ghofrani HA, Simonneau G, Rubin LJ. Riociguat for pulmonary hypertension [reply]. N Engl J Med 2013;369(23):2268.
7. Ryan JJ, Thenappan T, Luo N, Ha T, Patel AR, Rich S, Archer SL. The WHO classification of pulmonary hypertension: a case-based imaging compendium. Pulm Circ 2012;2(1):107–121.
8. Jenkins D, Mayer E, Screaton N, Madani M. State-of-the-art chronic thromboembolic pulmonary hypertension diagnosis and management. Eur Respir Rev 2012;21(123):32–39.
9. Heinrich M, Uder M, Tscholl D, Grgic A, Kramann B, Schäfers HJ. CT scan findings in chronic thromboembolic pulmonary hypertension: predictors of hemodynamic improvement after pulmonary thromboendarterectomy. Chest 2005;127(5):1606–1613.
10. Schölzel BE, Post MC, Van de Bruaene A, Dymarkowski S, Wuyts W, Meyns B, Budts W, Delcroix M. Prediction of hemodynamic improvement after pulmonary endarterectomy in chronic thromboembolic pulmonary hypertension using non-invasive imaging. Int J Cardiovasc Imaging 2015;31(1):143–150.
11. San José Estépar R, Ross JC, Krissian K, Schultz T, Washko GR, Kindlmann GL. Computational vascular morphometry for the assessment of pulmonary vascular disease based on scale-space particles. 2012 9th IEEE International Symposium on Biomedical Imaging: from nano to macro. Proceedings. Piscataway, NJ: IEEE, 2012:1479–1482.
12. San José Estépar R, Kinney GL, Black-Shinn JL, Bowler RP, Kindlmann GL, Ross JC, Kikinis R, et al. Computed tomographic measures of pulmonary vascular morphology in smokers and their clinical implications. Am J Respir Crit Care Med 2013;188(2):231–239.
13. Pellegrini P, Rossi A, Pasotti M, Raineri C, Cicoira M, Bonapace S, Dini FL, et al. Prognostic relevance of pulmonary arterial compliance in patients with chronic heart failure. Chest 2014;145(5):1064–1070.
14. Wells JM, Iyer AS, Rahaghi FN, Bhatt SP, Gupta H, Denney TS, Lloyd SG, et al. Pulmonary artery enlargement is associated with right ventricular dysfunction and loss of blood volume in small pulmonary vessels in chronic obstructive pulmonary disease. Circ Cardiovasc Imaging 2015;8(4):e002546. doi:10.1161/CIRCIMAGING.114.002546.
15. Wells JM, Washko GR, Han MK, Abbas N, Nath H, Mamary AJ, Regan E, et al. Pulmonary arterial enlargement and acute exacerbations of COPD. N Engl J Med 2012;367(10):913–921.
16. Hart WE, Goldbaum M, Côté B, Kube P, Nelson MR. Measurement and classification of retinal vascular tortuosity. Int J Med Inf 1999;53(2–3):239–252.
17. Bullitt E, Gerig G, Pizer SM, Lin W, Aylward SR. Measuring tortuosity of the intracerebral vasculature from MRA images. IEEE Trans Med Imaging 2003;22(9):1163–1171.
18. Bracher D. Changes in peripapillary tortuosity of the central retinal arteries in newborns: a phenomenon whose underlying mechanisms need clarification. Graefes Arch Clin Exp Ophthalmol 1982;218(4):211–217.
19. Han HC. Twisted blood vessels: symptoms, etiology and biomechanical mechanisms. J Vasc Res 2012;49(3):185–197.
20. Helmberger M, Pienn M, Urschler M, Kullnig P, Stollberger R, Kovacs G, Olschewski A, Olschewski H, Bálint Z. Quantification of tortuosity and fractal dimension of the lung vessels in pulmonary hypertension patients. PloS ONE 2014;9:e87515. doi:10.1371/journal.pone.0087515.